Adaptive Beam-Forming with Interference Suppression and Multi-User Detection in Satellite Systems with Terrestrial Reuse of Frequencies

Dunmin Zheng and Peter D. Karabinis

Mobile Satellite Ventures, LP

10802 Parkridge Blvd., Reston, VA 20191, USA

dzheng@msvlp.com; pkarabinis@msvlp.com

Abstract— **Adaptive space-time signal processing comprising interference suppression and multi-user detection in a CDMA Mobile Satellite System (MSS) environment is presented. Optimum beam-forming, based on a Minimum Mean-Squared Error (MMSE) performance index, is used to maximize the signal-to-noise plus interference ratio of MSS links in an environment of significant terrestrial reuse of the satellite service link frequencies by Ancillary Terrestrial Components (ATCs). The technique substantially mitigates both ATC-induced co-channel interference and Multiple-Access Interference (MAI). At the satellite gateway, a pilot-based MMSE algorithm is used to adaptively form an optimum return-channel beam for each user by processing the raw antenna feed element signals provided to the satellite gateway by a satellite return feeder link. Following beam-forming, pilot signals are used to estimate the multi-user channels. The proposed Sequential ATC and MAI Interference Canceller (SAMIC) algorithm takes advantage of *a priori* known pilot signal information and invokes preliminary decisions to sequentially perform interference suppression followed by multi-user detection. The performance of the SAMIC algorithm is illustrated by simulation of a multi-beam geo-stationary satellite system containing a wide deployment of ATC over 50 major markets across the Continental United States (CONUS).**

***Keywords*—Adaptive Beamforming, CDMA, Mobile Satellite System, Ancillary Terrestrial Component, Interference Cancellation, Multi-User Detection**

I. INTRODUCTION

The terrestrial reuse of satellite-band service-link frequencies is a relatively new concept that has been proposed to, and accepted by, the Federal Communications Commission (FCC)[1] and Industry Canada (IC).[2] In this paper, we analyze a hybrid system that is based on this new spectrally-efficient concept. The "Ancillary Terrestrial Component" (ATC) network reuses the satellite-band service link frequencies to provide reliable communications in populous areas, where satellite connectivity is unreliable, while the space segment serves rural and other non-populous areas. As a consequence, uplink co-channel interference to satellite links may be present and may become harmful, under certain conditions where there is insufficient discrimination between co-channel satellite and terrestrial links. In this paper we study the impact on a state-of-the-art Mobile Satellite System (MSS) of an ATC Network (ATN) that is widely deployed over 50 major markets spanning the Continental United States (CONUS).[3] The air interface communications protocol assumed for the system (for both the satellite and ATC service links) is cdma2000 1XRTT in accordance with the cdma2000-1XRTT specifications [1]. While the terrestrial part of the system (the ATC links) will experience interference in accordance with the conventional (well-understood) propagation impairments, the satellite part of the system (the satellite links) will, in general, experience additional ATC-induced co-channel interference. This additional ATC-induced interference on top of the conventional inter-beam and intra-beam Multiple-Access Interference (MAI) presents a new challenge for the CDMA-based hybrid satellite system.

In conventional third generation CDMA systems, the major impediments to signal detection are multipath fading and MAI. While the multipath fading can be effectively combated by rake matched filtering, through coherently combining of resolvable multipath replicas of the desired signal, the problem of MAI can be resolved with multi-user detection techniques [2][3]. Rake matched filtering is a time-domain signal processing technique, as is multi-user detection. To further improve receiver performance, space-domain processing techniques have been explored by using multiple antennas at the base station receiver. The gain due to space-domain processing is achieved by coherently combining the desired signals from multiple antennas. Combining space-domain techniques with time domain techniques, (space-time detection) [4], promises to significantly improve the capacity of CDMA systems. For the MSS environment, no known published work has postulated space-time detection to mitigate both MAI and strong co-channel interference.

Modern MSS satellites use multiple receiving antenna feed elements to form a plurality of service area spot-beams (or cells). Satellite systems such as that of Thuraya and Inmarsat-4, for example, process the signals provided by the satellite's receiving antenna feed elements at the satellite, by applying complex weights and then forming linear combinations thereof, to form a plurality of service area beams (cells). In contrast, the received antenna feed element signals may be transported to a satellite gateway, via one or more satellite feeder links, and processed there in accordance with one or more performance criteria. The present work, based on this approach, uses the satellite's antenna feed element signals to first perform adaptive beam-forming (in order to mitigate the ATN-induced interference and other interference) and then, operating on the reduced-interference signals, removes intra-beam MAI by resorting to multi-user detection. The space processing (beam-forming) is performed ahead of the time processing because it may be difficult to perform effective signal detection without first stripping-away the intra-system ATN-induced interference, which may be strong. The adaptive beam-former uses *a priori* knowledge

[1] *See* Report and Order and Notice of Proposed Rulemaking, FCC 03-15, *Flexibility for Delivery of Communications by Mobile Satellite Service Providers in the 2 GHz Band, the L-Band, and the 1.6/2.4 Bands,* IB Docket No. 01-185, Adopted: January 29, 2003, Released: February 10, 2003.

[2] *See* Industry Canada, Spectrum Management and Telecommunications Policy DGTP-006-04 "Spectrum and Licensing Policy to Permit Ancillary Terrestrial Mobile Services as Part of Mobile-Satellite Service Offerings," May 2004.

[3] The term ATC denotes the part of the overall ancillary terrestrial network that serves a specific market/city. The term ATN relates to the entire ancillary terrestrial network over the entire footprint of the satellite.

of the pilot signal of the cdma2000 reverse link waveform. Following the beam-forming, pilot signals are used to estimate multi-user channels for intra-beam MAI cancellation.

II. System Model

The satellite forward service links (space-to-earth) are assumed to exist over fixed spot beams. Each of the fixed forward link spot beams is analogous to a terrestrial cell though significantly larger. A three-cell frequency reuse cluster size is assumed for the forward satellite links, as depicted in Fig. 1. A number of ATC base stations (ancillary terrestrial cells) may exist within a satellite spot beam. The ATC base stations and the terminals thereof use frequencies that are allocated to adjacent satellite spot beams in order to maximize the isolation between the terrestrial and satellite reuse of the MSS spectrum. Fig. 1 also shows "exclusion" zones (dotted circles) inside of which the frequencies used for MSS are not made available to the ATC contained therein. Fig. 1 also illustrates the typically larger geographic footprints of the return-link satellite antenna feed elements (relative to the smaller footprints of the forward-link satellite spot-beams). The signals provided to the satellite gateway by such return-link antenna feed elements are used to perform optimum adaptive (return-link) signal processing comprising beam-forming, interference cancellation, channel estimation and multi-user detection.

The satellite channel is assumed to be Rician flat-fading. For the k^{th} return-link satellite user, the vector channel impulse response across L antenna feed elements may be written as

$$\mathbf{h}_k(\tau,t) = \mathbf{a}_k(\theta_k,\varphi_k)\beta_k(t)\delta(\tau-\tau_k) \qquad (1)$$

where

$$\mathbf{a}_k(\theta_k,\varphi_k) = [a_{k,1}(\theta_k,\varphi_k),\cdots a_{k,L}(\theta_k,\varphi_k)]^T \quad \in C^{Lx1} \qquad (2)$$

is the satellite return-link antenna feed element complex response vector for the k^{th} user located at elevation angle θ_k and azimuth angle φ_k. The quantity

$$\beta_k(t) = \rho_k \exp\{j(2\pi f_k t + \psi_k)\} \qquad (3)$$

is the return-link path gain for the k^{th} user, f_k is the Doppler shift and Ψ_k is a phase shift. The quantity τ_k in (1) represents a time delay of the k^{th} user. Assuming K co-beam users and the channel vector

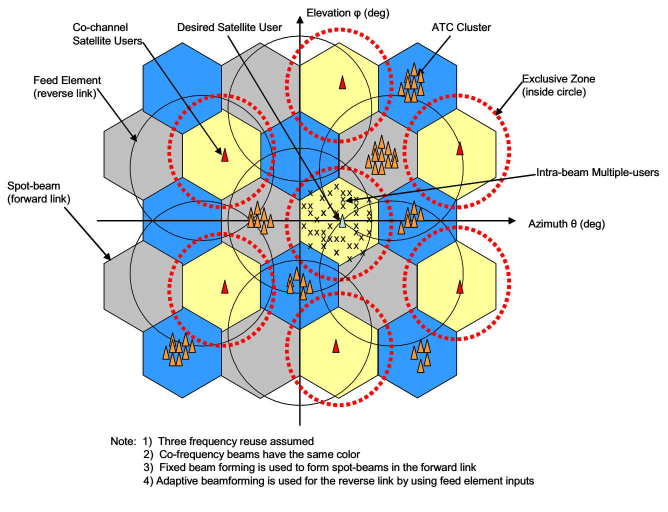

Figure 1. Satellite Forward-Link Beams and ATC Frequency Reuse

impulse response identified above, the data vector over the output of L antenna feed elements can be expressed as

$$\begin{aligned}\mathbf{y}(t) &= \sum_{k=1}^{K}[g_s b_k(t) s_k(t) + g_p p_k(t)] * \mathbf{h}_k(\tau,t) + \sum_{n=1}^{N}\mathbf{a}_n(\theta_n,\varphi_n) g_n v_n(t) + \mathbf{n}(t) \quad \in C^{Lx1} \\ &= \sum_{k=1}^{K}[\mathbf{a}_k(\theta_k,\varphi_k)\beta_k(t) g_s b_k(t-\tau_k) s_k(t-\tau_k) + \mathbf{a}_k(\theta_k,\varphi_k)\beta_k(t) g_p p_k(t-\tau_k)] \\ &\quad + \sum_{n=1}^{N}\mathbf{a}_n(\theta_n,\varphi_n) g_n v_n(t) + \mathbf{n}(t)\end{aligned} \qquad (4)$$

where $b_k(t)$ and $s_k(t)$ denote the information bit and spreading sequence, respectively, of the k^{th} user with M chips/bit; $p_k(t)$ is the pilot chip sequence of the k^{th} user; and g_s and g_p denote amplitudes of the traffic data signal and the pilot signal, respectively (assumed the same for all K users). The quantity $v_n(t)$ denotes the aggregate interference signal generated by the n^{th} ATC service area/city modeled as complex Gaussian noise, and g_n is associated amplitude. Finally, $\mathbf{n}(t) \in C^{Lx1}$ represents additive complex Gaussian noise.

Assuming matched filtering by correlating the signal that is received by the l^{th} antenna feed element with the information and pilot spreading codes, an M-vector output signal corresponding to the l^{th} antenna feed element can be expressed as

$$\mathbf{y}_l = \sum_{k=1}^{K}[a_{k,l}(\theta_k,\varphi_k)\beta_k(g_s b_k \mathbf{s}_k + g_p \mathbf{p}_k)] + \sum_{n=1}^{N} a_{n,l}(\theta_n,\varphi_n) g_n \mathbf{v}_n + \mathbf{n}_l \quad \in C^{Mx1} \qquad (5)$$

where $\mathbf{s}_k$ and $\mathbf{p}_k$ denote the spreading code M-vectors corresponding to $s_k(t-\tau_k)$ and $p_k(t-\tau_k)$ respectively. The spreading codes for the signal and pilot are normalized and are assumed orthogonal $\|\mathbf{s}_k\| = 1$, $\|\mathbf{p}_k\| = 1$; $\langle \mathbf{s}_k, \mathbf{p}_k \rangle = 0$; $\mathbf{v}_n$ is the complex M-vector Gaussian noise corresponding to the n^{th} ATC service area, and $\mathbf{n}_l$ is a complex M-vector corresponding to the Gaussian noise at the l^{th} antenna feed element.

By introducing matrix notation, we may rewrite Equation (5) as:

$$\mathbf{y}_l = \mathbf{S}\,\mathbf{A}_l\,\mathbf{b}\,g_s + \mathbf{P}\,\mathbf{A}_l\,\mathbf{1}_K\,g_p + \mathbf{V}\,\mathbf{A}_l^{(n)}\,\mathbf{1}_N\,g_n + \mathbf{n}_l \qquad (6)$$

where $\mathbf{S} = [\mathbf{s}_1\ \mathbf{s}_2\ \cdots \mathbf{s}_K] \in C^{MxK} \equiv$ data spreading code matrix; $\mathbf{A}_l = \mathrm{diag}\{a_{1,l}(\theta_1,\varphi_1)\beta_1 \cdots a_{K,l}(\theta_K,\varphi_K)\beta_K\} \in C^{KxK} \equiv l^{th}$ feed element/channel matrix; $\mathbf{b} = [b_1 \cdots b_K]^T \in \mathcal{R}^{Kx1} \equiv K$-vector of data bits; $\mathbf{P} = [\mathbf{p}_1\ \mathbf{p}_2 \cdots \mathbf{p}_K] \in C^{MxK} \equiv$ pilot spreading code matrix; $\mathbf{1}_u = [1 \cdots 1]^T \in \mathcal{R}^{ux1} \equiv u$-vector of ones; $\mathbf{V} = [\mathbf{v}_1\ \mathbf{v}_2 \cdots \mathbf{v}_N] \in C^{MxN} \equiv$ ATC interference matrix; and $\mathbf{A}_l^{(n)} = \mathrm{diag}\{a_{1,l}(\theta_1,\varphi_1) \cdots a_{N,l}(\theta_N,\varphi_N)\} \in C^{NxN} \equiv l^{th}$ feed element matrix for N ATCs. The noise vector $\mathbf{n}_l \in C^{Mx1}$ is a zero-mean complex Gaussian vector. The ATC interference vector $\mathbf{v}_n \in C^{Mx1}$ (for the n^{th} ATC, $n = 1, 2, \cdots N$) is modeled as a zero-mean complex Gaussian vector, and g_n is assumed the same for all ATCs. Given the above formulation, the problem of interest is to estimate the information $b_k\ (k = 1, 2, \cdots K)$ from the observables $\mathbf{y}_l\ (l = 1, 2, \cdots L)$.

III. Multi-User Detector in Conjunction with ATC Interference Cancellation

3.1 Pilot-Based Spatial Channel MMSE Estimator

Let $\mathbf{z}_l^{(p)}$ be the *K*-vector complex output of a bank of *K* filters matched to a delayed set of pilot signals $\mathbf{p}_1\ \mathbf{p}_2 \cdots \mathbf{p}_K$. The input to the *K* filters is the signal provided by antenna feed element *l*. We assume that the timing estimate for each of the *K* users is obtained though a pilot searcher [5]. For the l^{th} element, the *K*-complex vector output from the *K* matched filters is the de-spread version of received signals, which is given by

$$\mathbf{z}_l^{(p)} = \mathbf{P}^H \mathbf{y}_l = \mathbf{R}^{(p)} \mathbf{A}_l \mathbf{1}_K g_p + \mathbf{R}^{(ps)} \mathbf{A}_l \mathbf{b} g_s + \mathbf{R}^{(pv)} \mathbf{A}_n \mathbf{1}_N g_n + \mathbf{P}^H \mathbf{n}_l \qquad \in C^{Kx1} \qquad (7)$$

where $(\cdot)^H$ denotes the complex conjugate transpose, and $\mathbf{R}^{(p)} = \mathbf{P}^H\mathbf{P} \quad \in C^{KxK}$ ≡ Pilot correlation matrix with ones along the main diagonal; $\mathbf{R}^{(ps)} = \mathbf{P}^H\mathbf{S} \quad \in C^{KxK}$ ≡ Pilot/signal cross-correlation matrix with zeros along the main diagonal; $\mathbf{R}^{(pv)} = \mathbf{P}^H\mathbf{V} \quad \in C^{KxN}$ ≡ Pilot/ATC cross-correlation matrix.

From Equation (7), we can derive the normalized de-spread pilot channel output vector:

$$\mathbf{d}_l^{(p)} = \frac{\mathbf{z}_l^{(p)}}{g_p} = \underbrace{\mathbf{A}\mathbf{1}_K}_{\text{(desired)}} + \underbrace{(\mathbf{R}^{(p)} - \mathbf{I}_k)\mathbf{A}\mathbf{1}_K + \mathbf{R}^{(ps)}\mathbf{A}\mathbf{b}\frac{g_s}{g_p}}_{\text{(MAI)}} + \underbrace{\mathbf{R}^{(pv)}\mathbf{A}_n\mathbf{1}_N\frac{g_n}{g_p}}_{\text{ATC interference}} + \underbrace{\frac{1}{g_p}\mathbf{P}^H\mathbf{n}_l}_{\text{Noise}} \qquad (8)$$

Assuming the channel responses do not change over a period of Q symbols, we can improve the pilot estimate by averaging Q successive instances of $\mathbf{d}_l^{(p)}$. In the simulation study, we will use the following approximation for the averaged estimate using long codes:

$$\hat{\mathbf{d}}_l^{(p)} = \frac{1}{Qg_p}\sum_{q=1}^{Q} \mathbf{z}_{l,q}^{(p)} \qquad (9)$$
$$= \mathbf{A}_l\mathbf{1}_K + \frac{1}{\sqrt{Q}}(\mathbf{R}^{(p)} - \mathbf{I}_k)\mathbf{A}_l\mathbf{1}_K + \frac{1}{\sqrt{Q}}\mathbf{R}^{(ps)}\mathbf{A}_l\mathbf{b}\frac{g_s}{g_p} + \frac{1}{\sqrt{Q}}\mathbf{R}^{(pv)}\mathbf{A}_n\mathbf{1}_N\frac{g_n}{g_p} + \bar{\mathbf{n}}_l$$

where the complex Gaussian noise term has distribution $\bar{\mathbf{n}}_l \sim \eta\{\mathbf{0}_K, g_p^{(-2)}\sigma^2\mathbf{R}^{(p)}/Q\}$.

Since the estimate of the pilot signal contains ATC interference and MAI, we will first remove ATC interference by processing the plurality of feed element signals and taking advantage of known pilot signal properties. We define the estimate of the k^{th} user's pilot vector across *L* feed elements as

$$\mathbf{y}_k^{(p)} = [\hat{\mathbf{d}}_1^{(p)}(k)\ \hat{\mathbf{d}}_2^{(p)}(k) \cdots \hat{\mathbf{d}}_L^{(p)}(k)]^T \qquad \in C^{Lx1} \qquad (10)$$

where $\hat{\mathbf{d}}_l^{(p)}$ is defined in (9). Now we are ready to derive the pilot-based MMSE interference canceller. The MMSE criterion attempts to minimize the difference between the output of the beam former and the desired user's response [6]. The MMSE interference canceller can be implemented with the computationally efficient Least Mean Square (LMS) adaptive algorithm:

$$\mathbf{w}_k(n+1) = \mathbf{w}_k(n) + \mu\,\mathbf{y}_k^{(p)}(n)\,e_k^*(n) \qquad \in C^{Lx1} \qquad (11)$$

where $e_k(n) = d_k(n) - \mathbf{w}_k^H(n)\,\mathbf{y}_k^{(p)}(n)$ is the error signal, and μ is the step-size coefficient. Applying the weight $\hat{\mathbf{w}}_k$ to the k^{th} user's pilot vector $\mathbf{y}_k^{(p)}$ provides an estimate of the pilot symbol after adaptive beam forming and ATC interference suppression:

$$\hat{p}_{(symb)k} = \hat{\mathbf{w}}_k^H\mathbf{y}_k^{(p)} = \hat{\mathbf{w}}_k^H[\hat{\mathbf{d}}_1^{(p)}(k)\ \hat{\mathbf{d}}_2^{(p)}(k) \cdots \hat{\mathbf{d}}_L^{(p)}(k)]^T = \sum_{l=1}^{L}\hat{\mathbf{w}}_k^H(l)\hat{\mathbf{d}}_l^{(p)}(k) \qquad (12)$$

3.2 ATC Interference Cancellation

The resulting weight $\hat{\mathbf{w}}_k$ minimizes the ATC co-channel interference plus thermal noise based on processing of the pilot signal. Since the pilot signal and the traffic signal are received through the same feed element and propagation channel, the estimated weight $\hat{\mathbf{w}}_k$ can also be applied to the traffic signal as well. Unlike ATC interference, multiple access interference (MAI) is interference that cannot be removed by spatial processing techniques. We have developed a new algorithm to ensure an efficient removal of MAI after ATC interference cancellation. The chip level beam-formed signal can be obtained by applying the weight $\hat{\mathbf{w}}_k^H$ in (11) to $\mathbf{y}_l$ in (6)

$$\mathbf{r}_k = \sum_{l=1}^{L}(\hat{\mathbf{w}}_k^H)_l\mathbf{y}_l \qquad \in C^{Mx1}$$
$$= \sum_{l=1}^{L}(\hat{\mathbf{w}}_k^H)_l\mathbf{S}\,\mathbf{A}_l\,\mathbf{b}g_s + \sum_{l=1}^{L}(\hat{\mathbf{w}}_k^H)_l\,\mathbf{P}\,\mathbf{A}_l\,\mathbf{1}_K\,g_p + \sum_{l=1}^{L}(\hat{\mathbf{w}}_k^H)_l\mathbf{V}\mathbf{A}_l^{(n)}\mathbf{1}_N g_n + \sum_{l=1}^{L}(\hat{\mathbf{w}}_k^H)_l\mathbf{n}_l$$
$$= \mathbf{S}\tilde{\mathbf{A}}_k\mathbf{b}g_s + \mathbf{P}\tilde{\mathbf{A}}_k\mathbf{1}_K g_p + \mathbf{V}\tilde{\mathbf{A}}_k^{(n)}\mathbf{1}_N g_n + \tilde{\mathbf{n}}_k \qquad (13)$$

where $\tilde{\mathbf{A}}_k = \sum_{l=1}^{L}(\hat{\mathbf{w}}_k^H)_l\mathbf{A}_l$, $\tilde{\mathbf{A}}_k^{(n)} = \sum_{l=1}^{L}(\hat{\mathbf{w}}_k^H)_l\mathbf{A}_l^{(n)}$, $\tilde{\mathbf{A}}_k^{(n)} = \sum_{l=1}^{L}(\hat{\mathbf{w}}_k^H)_l\mathbf{A}_l^{(n)}$, and $\tilde{\mathbf{n}}_k = \sum_{l=1}^{L}(\hat{\mathbf{w}}_k^H)_l\mathbf{n}_l$.

Note that this beam-formed signal for the k^{th} user is just the ATC cancelled signal, but still has MAI which is contributed from the other *K-1* co-beam/co-frequency users.

As shown in Fig. 2, the interference canceller for the k^{th} user is a spatial combiner by using $\hat{\mathbf{w}}_k$ as in (13) followed by the correlator $\mathbf{s}_k$. The interference cancelled bit estimate can be obtained by

$$\hat{b}_k = \mathrm{Sgn}\left(x_k^{(s)}\right) \qquad (14)$$

where

$$x_k^{(s)} = \mathrm{Re}\left(\mathbf{s}_k^H\mathbf{r}_k\right) \qquad (15)$$

3.3 Channel Estimation

Given that we already have accomplished ATC interference cancellation and single-user detection, as well as timing and formed-beam/channel estimates, we are able to reconstruct the MAI and subtract it from the signal. To reconstruct the MAI, we first need to estimate the channel for each user by using the pilot signals. We apply the beam-formed signal $\mathbf{r}_k$ to a bank of *K* filters matched to the users' delayed pilot signals $\mathbf{p}_1\ \mathbf{p}_2 \cdots \mathbf{p}_K$.

$$\tilde{\mathbf{z}}_k^{(p)} = \mathbf{P}^H\mathbf{r}_k = \mathbf{R}^{(p)}\tilde{\mathbf{A}}_k\mathbf{1}_k g_p + \mathbf{R}^{(ps)}\tilde{\mathbf{A}}_k\mathbf{b}g_s + \mathbf{R}^{(pv)}\tilde{\mathbf{A}}_k^{(n)}\mathbf{1}_N g_n + \mathbf{P}^H\tilde{\mathbf{n}}_k \qquad \in C^{Kx1} \qquad (16)$$

Letting the *K*-vector $\hat{\boldsymbol\alpha}_k = [\,\hat\alpha_{k,1}\ \ \hat\alpha_{k,2}\ \cdots\ \hat\alpha_{k,K}\,]^T \quad \in C^{Kx1}$ denote the relevant channel estimates associated with the k^{th} user, $\hat{\boldsymbol\alpha}_k$ can be obtained by normalizing $\tilde{\mathbf z}_k^{(p)}$ by the pilot amplitude g_p. The channel estimates may be further improved by integrating over a period of Q pilot symbols so that the ATC interference residue and MAI (as well as the noise) are low-pass filtered.

3.4 Sequential ATC and MAI Interference Cancellation (SAMIC) Detector

We can reconstruct the MAI due to all interferers $(j = 1 \ldots K,\ j \neq k)$ by using corresponding formed beam/channel estimates $(\hat\alpha_{k,j}, j \neq k)$ and bit estimates $(\hat b_j, j \neq k)$, and subtract the reconstructed MAI from the beam-formed signal $\mathbf r_k$.

The sequential ATC and MAI Interference Cancellation (SAMIC) detector is based on the idea that cancellation of MAI may be accomplished efficiently following ATC interference cancellation. The SAMIC detector uses modified signals that are obtained by subtracting the estimated and reconstructed MAI from the beam-formed signals:

$$\tilde{\mathbf r}_k = \mathbf r_k - \sum_{j=1,j\neq k}^{K} \hat\alpha_{k,j}\mathbf s_j g_s \hat b_j \qquad \in C^{Mx1} \qquad (k=1..K) \tag{17}$$

where the channel estimates $\hat{\boldsymbol\alpha}_k$ are obtained from the pilot channel after beam-forming, and the bit estimates are obtained in (14) from single-user detection after beam-forming. Submitting $\hat{\boldsymbol\alpha}_k$ and $\hat b_j$, $\mathbf s_j$ $(j \neq k)$ to (17) yields $\tilde{\mathbf r}_k$. The MAI-removed $\tilde{\mathbf r}_k$ is followed by the correlator that is matched to the spreading code $\mathbf s_k$; we obtain the maximum-likelihood detector for the k^{th} user as follows:

$$\mathbf s_k^H \tilde{\mathbf r}_k = \mathbf s_k^H \mathbf S \tilde{\mathbf A}_k \mathbf b g_s + \mathbf s_k^H \mathbf P \tilde{\mathbf A}_k \mathbf 1_K g_p + \mathbf s_k^H \mathbf V \tilde{\mathbf A}_k^{(n)} \mathbf 1_N g_n + \bar n_k - \sum_{j=1,j\neq k}^{K} \hat\alpha_{k,j}\rho_{k,j} g_s \hat b_j \tag{18}$$

where

$$\rho_{k,j} = \mathbf s_k^H \mathbf s_j, \quad (k \neq j) \tag{19}$$

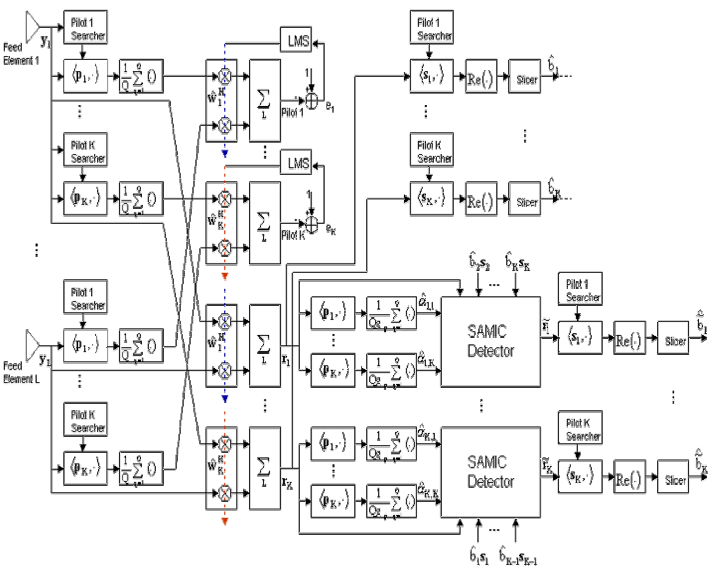

Figure 2. Interference Canceller and Multi-User Detector

$$\bar n_k = \mathbf s_k^H \bar{\mathbf n}_k = \mathbf s_k^H \sum_{l=1}^{L} (\hat{\mathbf w}_k^H)_l \mathbf n_l \tag{20}$$

The slicer input for the SAMIC detector is

$$\tilde x_k^{(s)} = \mathrm{Re}\left(\mathbf s_k^H \tilde{\mathbf r}_k\right) = \gamma_k g_s + \varepsilon_k g_p + \nu_k g_n + \tilde n_k - \delta_k g_s \tag{21}$$

where

$$\gamma_k = \mathrm{Re}\left(\mathbf s_k^H \mathbf S \tilde{\mathbf A}_k \mathbf b\right) \tag{22}$$

$$\varepsilon_k = \mathrm{Re}\left(\mathbf s_k^H \mathbf P \tilde{\mathbf A}_k \mathbf 1_K\right) \tag{23}$$

$$\nu_k = \mathrm{Re}\left(\mathbf s_k^H \mathbf V \tilde{\mathbf A}_k^{(n)} \mathbf 1_N\right) \tag{24}$$

$$\delta_k = \mathrm{Re}\left(\sum_{j=1,j\neq k}^{K} \hat\alpha_{k,j}\rho_{k,j}\hat b_j\right) \tag{25}$$

$$\tilde n_k = \mathrm{Re}\left(\bar n_k\right) \tag{26}$$

The final decision for the interference cancelled symbol/bit is the output of the slicer:

$$\hat{\hat b}_k = \mathrm{sgn}\left(\tilde x_k^{(s)}\right) \tag{27}$$

The noise term apparently has the statistics distribution: $\tilde n_k \sim \eta\left(0, \|\hat{\mathbf w}_k\|^2 \sigma^2\right)$.

IV. SIMULATION RESULTS

In this section, we present simulation results illustrating the performance of the ATC interference canceller and the SAMIC detector. The simulation is based on realistic satellite feed element gain/phase profiles that have been provided by a major satellite manufacturer. Fig. 3 illustrates the locations of the ATC (dots) over CONUS and the contours (footprints) of the return-link antenna feed elements. Fig. 4 presents performance of ATC-induced interference suppression as a function of "Satellite Signal to ATC Power ratio that is launched toward satellite" (*SIR*). The ATC Power that is launched toward the satellite is the aggregate co-channel power that is generated by all surviving ATCs after exclusion zone elimination (there are 16 such ATCs). In Fig. 4, each surviving ATC is treated as a point source interferer and all surviving ATCs are assumed to generate equal co-channel power. The desired satellite signal (terminal) is assumed to be at the center of feed element #21 (see Fig. 3). The parameter in Fig. 4 is the number of antenna feed elements ("receivers") that are processed. It is seen that performance gains diminish beyond 17 feed elements since, in this scenario, there are only 16 ATC locations providing interference.

The return link adaptive beam-forming generates an optimal beam to "null-out" as many sources of interference (ATCs) as possible. The adaptively generated weights form a beam that creates a null for each ATC interferer as long as there are sufficient degrees of freedom. Fig. 5 shows the adaptively formed beam pattern gain contours with the ATC distribution. In the contour plots, each contour ring represents 10 dB of gain reduction from the very next inner contour. The effect of interference cancellation is clearly demonstrated by the adaptive beam-forming.

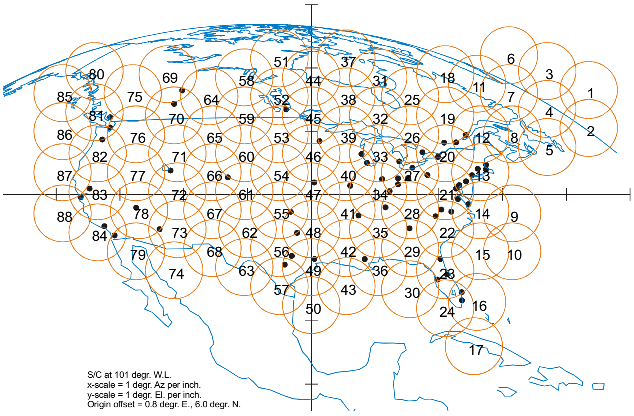

Figure 3. Footprint of Antenna Feed Elements and ATC Distribution over CONUS

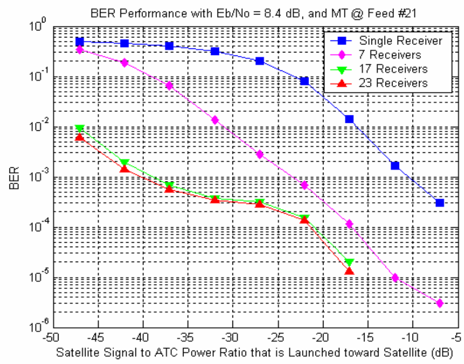

Figure 4. Impact of Number of Feed Elements on *BER* Performance

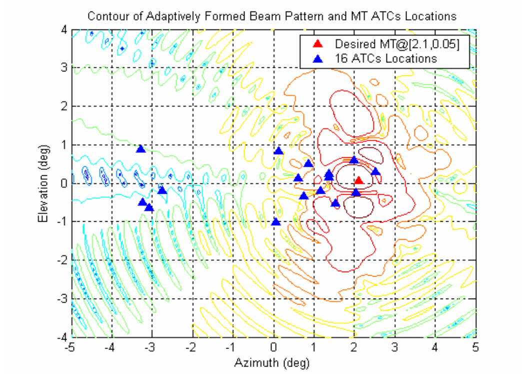

Figure 5. Contour of Adaptively Formed Beam Pattern and MT/ATC Locations (with 17 feed elements)

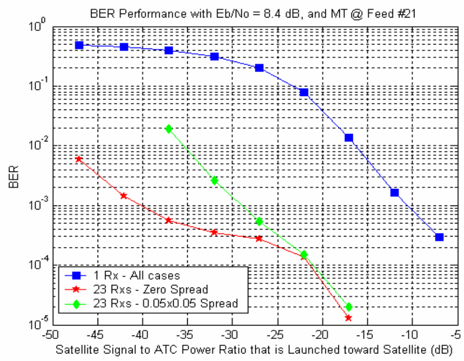

Figure 6. Impact on Canceller Performance of ATC Spread

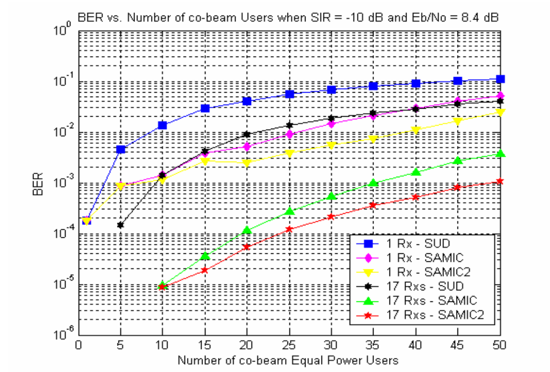

Figure 7. Average *BER* vs. Number of Co-Beam Users; Spreading Gain $M = 64$

Fig. 6 illustrates the impact on performance of having "spread" the power that is associated with each point-source ATC over a geographic area of 25 x 25 miles reflecting the size of a city.

With interference cancellation performance as depicted in Fig. 4, the performance of the SAMIC/SAMIC2 detector (multi-user detection) and SUD (Single User Detection) detector is illustrated in Figure 7 as a function of the number of co-beam users at *SIR* = -10 dB with a spreading gain of 64. It is seen from Fig. 7 that at *SIR* = -10 dB, over 44 co-beam users may communicate over a single CDMA carrier frequency while maintaining *BER* of 10^{-3}.

V. Conclusions

We have studied return-link adaptive optimum beam-forming in conjunction with multi-user detection for a satellite-based CDMA system with significant ATC-induced co-channel interference. A set of equations has been presented defining a new space-time receiver algorithm that, for each user, forms the optimum return-link satellite antenna pattern (beam) for mitigating ATC-induced interference and enables efficient multiple access detection. Several simulation examples have been presented illustrating the combined utility of ATC-induced interference cancellation followed by multi-user detection via the new SAMIC algorithm.

Acknowledgment

This work would not have been possible without the rare intellect of Gary Parsons and Dr. Rajendra Singh who invented ATC and recognized its enormous potential. Their vision is creating a new paradigm for MSS. Also, the wisdom of the many dedicated people at the Federal Communications Commission and at Industry Canada who studied and embraced the concept of ATC is acknowledged and commended.

References

[1] 3GPP2, "Physical Layer Standard for cdma2000 Spread Spectrum Systems", C.S0002-D, Version 1.0, February, 2004.
[2] S. Verdú, *Multiuser Detection*, Cambridge University Press, 1998.
[3] M.K. Varanasi and B. Aazhang, "Multistage Detection in Asynchronous Code-Division Multiple-Access Communications," *IEEE Transactions on Communications,* Vol. 38, No. 4, pp. 509-519, April 1990.
[4] M. Nagatsuka and R. Kohno, "A Spatially and Temporally Optimal Multi-User Receiver Using an Array Antenna for DS/CDMA," *IEICE Trans. on Communications*, Vol. E78-B, No. 11, Nov. 1995.
[5] D. Zheng, J. Li, S. Miller, and E. Strom, "An Efficient Code-Timing Estimator for DS-CDMA Signals," *IEEE Transactions on Signal Processing*, Vol. 45, No. 1, pp. 82-89, Jan. 1997.
[6] B. Widrow and S. Sterns, *Adaptive Signal Processing*, Prentice-Hall, New Jersey, 1985.